Am J Transl Res 2026;18(5):4516-4524
www.ajtr.org /ISSN:1943-8141/AJTR0170457

Original Article

Diagnostic performance of multimodal imaging integrating X-ray, CT, and MRI in femoroacetabular impingement syndrome

Qitong Liu, Weiguo Zhang, Yu Mu

Department of Radiology, Beijing Chao-Yang Hospital, Capital Medical University, Chaoyang District, Beijing 100021, China

Received December 2, 2025; Accepted April 23, 2026; Epub May 15, 2026; Published May 30, 2026

Abstract: Objective: To evaluate the diagnostic performance of combined X-ray, computed tomography (CT), and magnetic resonance imaging (MRI) for femoroacetabular impingement (FAI) syndrome and its subtypes, and to explore potential factors associated with FAI. Methods: A total of 86 patients with FAI syndrome (FAI group) and 70 individuals without hip joint abnormalities (control group) were retrospectively enrolled. All participants underwent X-ray, CT, and MRI examinations. The imaging findings were collected and analyzed. The diagnostic performance of each modality and their combination for FAI syndrome was analyzed using the receiver operating characteristic (ROC) curve analysis. Subsequently, independent risk factors were identified, and a nomogram prediction model was built and validated. Results: The area under the ROC curve (AUC) for diagnosing FAI syndrome using X-ray, CT, and MRI was 0.792, 0.845, and 0.889, respectively, whereas the combined diagnostic model achieved an AUC of 0.932 (specificity: 90.70%, sensitivity: 95.71%, accuracy: 92.95%). Multivariate analysis further identified age, high-intensity exercise history (Hx_HIE), α angle, and center-edge (CE) angle as independent risk factors for FAI syndrome, while femoral offset played a protective role. The constructed nomogram demonstrated excellent predictive performance, with a C-index of 0.966 and high calibration accuracy, particularly in the high-risk range. Conclusion: The joint screening using X-ray, CT, and MRI can significantly improve the diagnostic accuracy for FAI syndrome. Age ≥32 years, a history of high-intensity exercise, increased α/CE angles, and decreased femoral offset are associated with a higher risk of developing FAI syndrome.

Keywords: X-ray, CT, MRI, femoroacetabular impingement, subtypes, risk factor

Introduction

Femoroacetabular impingement (FAI) syndrome is a common cause of hip pain and a risk factor for the development of hip osteoarthritis and total hip replacement in young individuals [1]. This condition is primarily caused by abnormal morphology of the proximal femur and/or acetabulum, leading to abnormal contact between the acetabular rim and the femoral head-neck junction. Such impingement can be classified into three categories: cam, pincer, and mixed type [2].

Cam deformity, with a prevalence of approximately 37%, is characterized by an aspheric femoral head and associated with abnormal bone growth at the head-neck junction [3]. Pincer morphology, with a prevalence of about 67%, is closely associated with acetabular retroversion [4]. The mixed type is more common than the first two subtypes and presents anatomical features of both cam and pincer deformities [5].

According to statistics, the diagnostic rate of FAI syndrome has shown a significant upward trend in recent years, particularly among young people and athletes. Consequently, the number of related arthroscopic procedures has also surged [6]. Although the surgical strategies for FAI syndrome have been continuously optimized, and early surgical intervention often leads to better outcomes, timely diagnosis remains challenging [7]. This is related to the subtle clinical manifestations and mild struc-

https://doi.org/10.62347/LBAX3884

tural abnormalities in many FAI patients, as well as the overlap of FAI-related symptoms with those of other musculoskeletal disorders (e.g., hip, pelvic, or lumbar spine disorders), which further complicates the diagnostic process [8].

X-ray is a widely used imaging modality capable of revealing internal skeletal structure, such as fractures, dislocations, osteopathies, and foreign bodies, thus realizing disease diagnosis [9]. Despite low cost, rapid acquisition, and wide availability, X-ray also shows the disadvantages of ionizing radiation exposure, low soft-tissue resolution, and limited capability in depicting complex three-dimensional anatomical structural [10]. Computed tomography (CT) and magnetic resonance imaging (MRI) are two other commonly used imaging techniques. CT mainly utilizes rotating X-ray beams and three-dimensional reconstruction to obtain detailed anatomical structure; however, it is associated with ionizing radiation exposure and has limited sensitivity in detecting soft-tissue injuries (e.g., cartilage and labral lesions) [11, 12]. MRI, on the other hand, provides more accurate information on soft-tissue structures by using magnetic fields and radiofrequency pulses to excite hydrogen proton signals. It offers the advantages of being radiation-free and providing excellent soft-tissue contrast. However, MRI is relatively time-consuming, costly, and has limited ability to depict microscopic cortical bone structure [13, 14].

At present, there are relatively few studies on the combined use of X-ray, CT, and MRI for screening FAI syndrome and analyzing different types and risk factors. Therefore, this study aims to explore the diagnostic performance of combined imaging modality of X-ray, CT, and MRI for FAI syndrome and to identify potential risk factors, thereby providing more reliable evidence for improving screening efficiency and risk stratification.

Information and methodology

Case selection

This retrospective study recruited 146 patients with FAI syndrome treated at our hospital between September 2021 and June 2025. All patients underwent X-ray, CT, and MRI examinations. This study was approved by the Ethics Committee of Beijing Chao-Yang Hospital, Capital Medical University.

Inclusion criteria: (1) diagnosis of FAI syndrome according to clinical manifestations and established diagnostic criteria [15]; while controls showed no hip joint abnormalities, no symptoms, with completely normal imaging findings; (2) age >18 years; (3) no contraindications to X-ray, CT, or MRI examinations; (4) receipt of arthroscopic minimally invasive surgery without contraindications; (5) no history of trauma or surgery to the affected hip joint; (6) presence of hip or groin pain; (7) imaging-confirmed morphological abnormalities at the femoral head-neck junction and acetabulum; (8) complete clinical data and routine detection indicators; (9) normal communication and cognitive abilities.

Exclusion criteria: (1) history of trauma, previous hip replacement, or other hip surgeries; (2) femoral head necrosis, synovitis, or coxotuberculosis; (3) pregnancy or lactation; (4) ankylosing spondylitis, rheumatoid arthritis, and other severe joint diseases; (5) malignancies or vital organ dysfunction; (6) congenital hip dysplasia.

Intervention methods

X-ray examination: patients underwent X-ray imaging using standard anteroposterior (AP) views of the pelvis and both hip joints, as well as 45°/90° Dunn views.

CT examination: CT scans were performed using Siemens SOMATOM Definition Flash CT scanner, with a conventional slice thickness of 5 mm. Bone window images were reconstructed at 0.625 mm and post-processed on a workstation to generate coronal, oblique axial, and three-dimensional reconstructions of the pelvis.

MRI examination: MRI was performed using a Discovery MR750w 3.0T system. The scanning parameters were as follows: T1WI sequence: FOV 300 mm × 280 mm, slice thickness 3.0 mm, TR 3384 ms, TE 82 ms; T2WI sequence: FOV 300 mm × 210 mm, slice thickness 3.5 mm, TR 650 ms, TE 10 ms; T2WI fat-suppressed sequence: FOV 210 mm × 210 mm, slice thickness 3.5 mm, TR 3962 ms, TE 32 ms. Representative MRI images are shown in **Figure 1**.

The X-ray, CT, and MRI images were evaluated independently and blindly by two radiologists

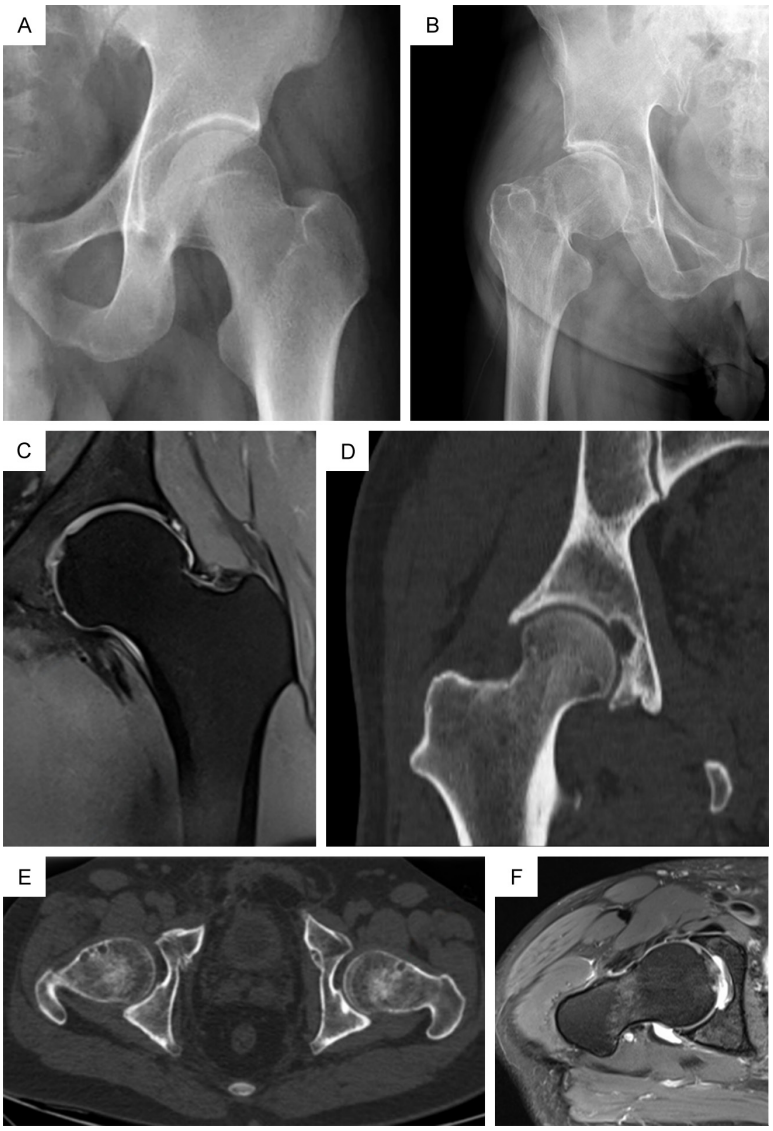

Figure 1. Representative MRI imaging findings. A. X-ray image of a normal hip joint showing preserved structure and normal joint space. B. X-ray image of a hip joint with abnormal bone hyperplasia and joint space alterations. C. 3D CT reconstruction of a control subject showing normal acetabular morphology and femoral head coverage. D. 3D CT reconstruction of a FAI patient clearly showing cam-type deformity of the femoral head. E. MRI of a control subject showing normal signal and intact soft tissues, including articular cartilage and acetabular labrum. F. MRI of a FAI patient showing typical soft tissue lesions caused by impingement, including labral tears and cartilage damage. Note: MRI, magnetic resonance imaging; FAI, femoroacetabular impingement; CT, computed tomography; 3D, three-Dimensional.

(associate director level or above). Discrepancies were resolved by consensus discussion.

Data collection

Diagnosis of FAI syndrome and its subtypes: FAI syndrome and its subtypes were diagnosed based on clinical manifestations and arthroscopic findings. A positive hip impingement test was considered indicative of FAI. Arthroscopically, cam type is characterized by a bony protrusion at the femoral head-neck junction, pincer type shows excessive acetabular coverage, and the mixed type exhibits characteristics of the above two, which may subsequently result in acetabular labral tears or cartilage damage [16].

Diagnostic data: The sensitivity (SEN), specificity (SPE), accuracy (ACC), as well as the positive (PPV) and negative predictive value (NPV) of three screening methods for FAI syndrome were calculated, using arthroscopic surgical records as the gold standard. These indexes were calculated as follows: SEN = true positives/(true positives + false negatives); SPE = true negatives/(false positives + true negatives); ACC = (true positives + true negatives)/total number of people tested; PPV = true positives/(true positives + false positives); NPV = true negatives/(false negatives + true negatives).

Other clinical data: Clinical information, including sex, age, body mass index (BMI), high-intensity exercise history (Hx_HIE), α angle, center-edge (CE) angle, and femoral offset, was extracted from patient medical records to analyze potential determinants of FAI syndrome.

Of these measures, FAI syndrome and its subtypes, as well as various diagnostic parameters, were primary outcomes, while other clinical data were treated as secondary outcomes.

Statistical methods

SPSS 25.0 was used for statistical analyses. Variance homogeneity and approximate normal

Table 1. Detection of FAI syndrome by X-ray, CT, and MRI

Imaging modality		Gold standard		Total
		Positive	Negative	
X-ray	Positive	60	8	68
	Negative	26	62	88
	Total	86	70	156
CT	Positive	68	7	75
	Negative	18	63	81
	Total	86	70	156
MRI	Positive	73	5	78
	Negative	13	65	78
	Total	86	70	156

Note: CT, computed tomography; MRI, magnetic resonance imaging; FAI, femoroacetabular impingement.

Table 2. Detection of FAI syndrome by joint modality

Joint detection	Gold standard		Total
	Positive	Negative	
Positive	78	3	81
Negative	8	67	75
Total	86	70	156

Note: FAI, femoroacetabular impingement.

distribution were evaluated using Bartlett's test and the Kolmogorov-Smirnov test, respectively. Continuous variables confirming to normal distribution were expressed as mean ± standard deviation ($\bar{x}$±sd), and differences between groups were examined using the independent sample t-tests. Categorical variables were presented as n (%) and compared between groups using the χ^2 test or the Fisher exact test, as appropriate. Receiver operating characteristic (ROC) curve analysis was performed to evaluate the diagnostic performance of the three imaging modalities for FAI syndrome, alone and in combination. Univariate and multivariate logistic regression analyses were conducted to identify potential risk factors associated with FAI syndrome. A nomogram predictive model was constructed based on independent risk factors. Internal validation of the model was performed using 1,000 bootstrap resamples, and predictive accuracy was assessed using calibration curves. A two-tailed *P* value <0.05 was considered statistically significant.

Results

Diagnosis of FAI syndrome by X-ray, CT, MRI, and their combination

X-ray screening identified 68 positive and 88 negative cases of FAI syndrome. CT detected 75 positive cases and 81 negative cases. MRI detected 78 positive cases and 78 negative cases. Their combined detection identified 81 positive cases and 75 negative cases (**Tables 1**, **2**).

Diagnostic performance of X-ray, CT, and MRI for FAI syndrome

ROC curve analysis showed that the AUC of X-ray for diagnosing FAI syndrome was 0.792 (95% CI: 0.719-0.865), with SPE, SEN, and ACC of 69.77%, 88.57%, and 78.21%, respectively. The AUC for CT screening was 0.845 (95% CI: 0.780-0.910), with 79.07% SPE, 90.00% SEN, and 83.97% ACC. MRI demonstrated an AUC of 0.889 (95% CI: 0.832-0.945), with an SPE of 84.88%, SEN of 92.86%, and ACC of 88.46%. The joint screening approach achieved the highest diagnostic performance, with an AUC of 0.932 (95% CI: 0.887-0.977), SPE of 90.70%, SEN of 95.71%, and ACC of 92.95% (**Figure 2**; **Table 3**).

Accuracy of X-ray, CT, and MRI in identifying FAI syndrome subtypes

For the diagnosis of cam, pincer, and mixed types of FAI syndrome, the diagnostic accuracy of X-ray was 82.61%, 80.00%, and 86.05%, respectively; the corresponding figures for CT were 91.30%, 90.00%, and 95.35%, respectively; and MRI achieved accuracies of 86.96%, 90.00%, and 93.02%, respectively. Notably, the joint modality achieved diagnostic accuracy of 95.65%, 95.00%, and 97.67% for cam, pincer, and mixed types, respectively (**Table 4**).

Univariate analysis of risk factors of FAI syndrome

Univariate analysis revealed that sex, age, BMI, Hx_HIE, α angle, CE angle, and femoral offset were significantly associated with FAI syndrome (all P<0.05), while hip trauma history and family history showed no marked association (P>0.05; **Table 5**).

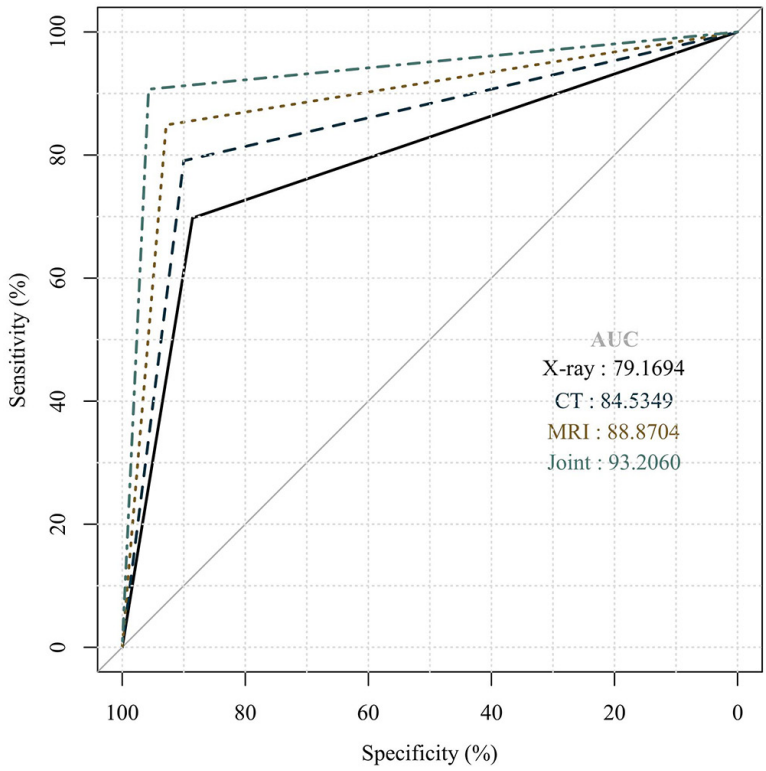

Figure 2. ROC curves for X-ray, CT, MRI, and their combination in diagnosing FAI syndrome. CT, computed tomography; MRI, magnetic resonance imaging; FAI, femoroacetabular impingement; AUC, areas under the curves.

Multivariate analysis of risk factors of FAI syndrome

Variables identified as significant in the univariate analysis were included in a binary logistic regression model for multivariate analysis. Gender and BMI were no longer statistically significant (P>0.05). However, age, Hx_HIE, α angle, CE angle, and femoral offset remained as independent predictors of FAI syndrome (all P<0.05; **Table 6**).

Nomogram construction and validation for predicting the risk of FAI syndrome

Based on the identified independent predictors (age, Hx_HIE, α angle, CE angle, and femoral offset), an individualized predictive nomogram for FAI syndrome was constructed. Bootstrap resampling (1000 iterations) was used for internal verification. The results demonstrated excellent discriminative ability, with a concordance index (C-index) of 0.966 (95% CI: 0.940-0.986). Analysis of the calibration curve revealed a slight overestimation in the low-risk interval, a minor underestimation in the medium-high risk interval, and high accuracy in the high-risk interval (**Figure 3**).

Discussion

The diagnostic value of X-ray, CT, and MRI in FAI syndrome has been extensively explored. Atalar et al. [17] reported that an X-ray-based deep-learning method improved the diagnostic efficiency in patients with suspected FAI presenting with hip pain. Ferrero et al. [18] reported that photon-counting CT is not only feasible in measuring α angle and acetabular version, but also offers advantages over energy-integrating detector CT by reducing the radiation dose by approximately 50%. Newhouse et al. [19] reported superiority of 3.0T MRI-based hip bone models over CT-assisted models in verifying FAI syndrome, possibly attributed to their higher resolution.

The findings of this study showed that the AUCs of X-ray, CT, and MRI for diagnosing FAI syndrome were 0.792, 0.845, and 0.889, respectively. Among the individual imaging modalities, MRI demonstrated the highest diagnostic performance, followed by CT and X-ray. The advantage of MRI may be related to its high sensitivity in detecting early structural and soft-tissue changes. MRI can also identify pathological findings such as bone marrow edema, acetabular labral tears, and cartilage abnormalities. However, due to limitations in spatial resolution, MRI may still face challenges in detecting subtle fissures in early cartilage lesions. When X-ray or CT diagnoses are inconclusive, MRI can directly reveal these crucial soft-tissue abnormalities, thereby playing a greater role in the early identification of FAI syndrome. Similarly, Xing et al. [20] reported that MRI exhibits superior performance in diagnosing ischiofemoral impingement syndrome. By measuring the ischiofemoral space and quadratus femoris

Table 3. Diagnostic performance of X-ray, CT, MRI, and their combination for FAI syndrome

Inspection means	AUC	Specificity	Sensitivity	Accuracy	Positive predictive value	Negative predictive value
X-ray	0.792	69.77%	88.57%	78.21%	88.24%	70.45%
CT	0.845	79.07%	90.00%	83.97%	90.67%	77.78%
MRI	0.889	84.88%	92.86%	88.46%	93.59%	83.33%
Joint detection	0.932	90.70%	95.71%	92.95%	96.30%	89.33%

Note: CT, computed tomography; MRI, magnetic resonance imaging; FAI, femoroacetabular impingement; AUC, areas under the curves.

Table 4. Accuracy of X-ray, CT, MRI and their combination in identifying FAI syndrome subsets

Examination modality	Cam type (n = 23)	Pincer type (n = 20)	Mixed type (n = 43)
X-ray	19 (82.61)	16 (80.00)	37 (86.05)
CT	21 (91.30)	18 (90.00)	41 (95.35)
MRI	20 (86.96)	18 (90.00)	40 (93.02)
Joint detection	22 (95.65)	19 (95.00)	42 (97.67)

Note: CT, computed tomography; MRI, magnetic resonance imaging; FAI, femoroacetabular impingement.

Table 5. Univariate analysis of risk factors for FAI syndrome

Data	Control group (n = 70)	FAI group (n = 86)	χ^2 value	*P* value
Sex			5.908	0.015
Female	38 (54.29)	30 (34.88)		
Male	32 (45.71)	56 (65.12)		
Age (years)			6.262	0.012
<32	45 (64.29)	38 (44.19)		
≥32	25 (35.71)	48 (55.81)		
Body mass index (kg/m^2)			7.980	0.005
<24	46 (65.71)	37 (43.02)		
≥24	24 (34.29)	49 (56.98)		
Hx_HIE			7.146	0.008
No	52 (74.29)	46 (53.49)		
Yes	18 (25.71)	40 (46.51)		
Hip trauma history			3.662	0.056
No	65 (92.86)	71 (82.56)		
Yes	5 (7.14)	15 (17.44)		
Family history				0.113
No	68 (97.14)	77 (89.53)		
Yes	2 (2.86)	9 (10.47)		
α angle (°)	47.73±7.61	63.62±10.86	10.345	<0.001
CE angle (°)	28.31±4.80	34.24±6.59	6.291	<0.001
Femoral offset (mm)	8.87±1.59	6.78±1.79	7.622	<0.001

Note: FAI, femoroacetabular impingement; Hx_HIE, high-intensity exercise history; CE angle, center-edge angle.

space, their diagnostic model achieved an AUC of approximately 0.950, which is consistent with our findings. Furthermore, Montin et al. [21] reported that three-dimensional MRI radiomics can distinguish patients with and without symptomatic FAI, and when combined with automatic joint segmentation techniques, it further improves the efficiency of FAI identification, providing additional support for our findings.

Table 6. Multivariate analysis of risk factors of FAI syndrome

Variable	B	Standard error	Wald	P	OR	95% CI
Sex	1.263	0.675	3.503	0.061	3.536	0.942-13.270
Age (years)	1.347	0.670	4.041	0.044	3.847	1.034-14.313
Body mass index (kg/m^2)	1.183	0.651	3.301	0.069	3.265	0.911-11.701
Hx_HIE	1.591	0.716	4.943	0.026	4.909	1.207-19.958
α angle (°)	0.285	0.064	19.570	<0.001	1.330	1.172-1.509
CE angle (°)	0.264	0.066	16.153	<0.001	1.302	1.145-1.480
Femoral offset (mm)	-0.702	0.207	11.536	0.001	0.496	0.331-0.743

Note: FAI, femoroacetabular impingement; Hx_HIE, high-intensity exercise history; CE angle, center-edge angle; OR, Odds Ratio; 95% CI, 95% Confidence Interval.

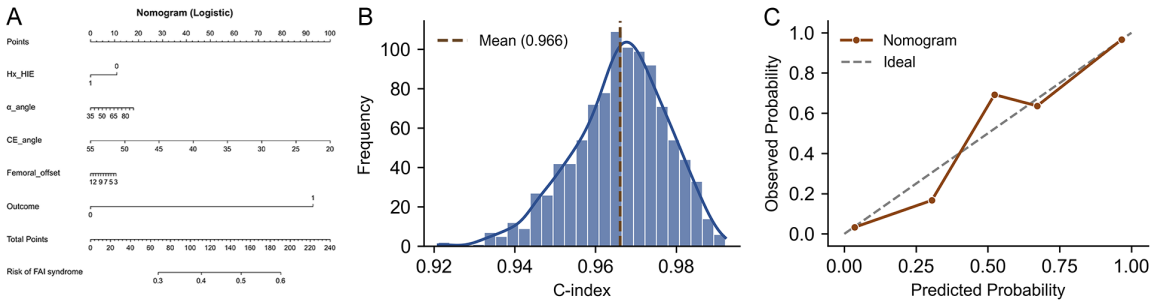

Figure 3. Nomogram construction for the risk of FAI syndrome and performance validation. A. Construction of the individualized predictive nomogram for FAI syndrome. B. Bootstrap resampling (n = 1000 iterations) of the model for internal validations. C. Calibration curves of the nomogram' predicted probabilities and actual outcomes. Note: FAI, femoroacetabular impingement; Hx_HIE, high-intensity exercise history; CE angle, center-edge angle; C-index, Concordance Index.

The combined imaging strategy achieved excellent diagnostic performance, with an AUC of 0.932, outperforming MRI and any single modality across all diagnostic indicators. These findings suggest that multimodal imaging integrating X-ray, CT, and MRI provides greater diagnostic efficiency for FAI syndrome. This may be due to the complementary strengths of the three modalities, which maximizes diagnostic performance. Specifically, X-rays has clear advantages in examining bone structures and can quickly identify obvious skeletal abnormalities. CT excels in accurately characterizing impingement morphology and quantifying structural parameters such as the α angles and femoral offsets. In contrast, MRI provides unique data in detecting clinically significant soft-tissue and early pathological changes, including bone marrow edema, labral tears, and cartilage damage caused by the bony abnormalities identified on CT. For instance, when CT shows a borderline α angle in patients with atypical symptoms, the corresponding bone marrow edema or labral tear indicated by MRI may serve as the key evidence supporting clinical intervention. Conversely, in patients with persistent symptoms but without obvious morphological abnormalities on X-ray or CT, MRI may reveal hidden labral injuries or early cartilage degeneration. Given these findings, the combined screening strategy is especially suitable for complex, atypical, or surgically planned cases, as it maximizes diagnostic accuracy and enhances the reliability of clinical decision-making.

In the study of Hayashi et al. [22], the combination of CT with anterior CE and α angles maximized the diagnostic efficiency for FAI syndrome (AUC = 0.920), though slightly lower than that observed in the present study. Additionally, the accuracy assessment for different subtypes of FAI syndrome yielded similar results. Multimodal imaging combining X-ray, CT, and MRI demonstrated the highest accuracy (95.65%, 95.00%, and 97.67% for cam, pincer, and mixed types, respectively) compared to any single imaging modality. Furthermore,

regression analysis identified age, Hx_HIE, α angle, CE angle, and femoral offset as independent predictors of FAI syndrome. Specifically, age of ≥32 years, the presence of Hx_HIE, increased α and CE angles, and reduced femoral offset were associated with an elevated risk of developing FAI syndrome. Patients aged 32 or above may have a reduced tolerance of the hip joint to abnormal stress due to cumulative microtrauma from long-term physical activity or occupational loading. In addition, aging-related degeneration and the diminished self-repair ability of articular cartilage may predispose them to FAI syndrome. A history of high-intensity exercise often reflects previous high-load hip joint movements, which may produce repeated stress close to the physiological limit at the femoral head-neck junction and the acetabular labrum. Over time, such repetitive stress may promote adaptive bony remodeling while simultaneously causing micro-trauma accumulation to the acetabular labrum, thereby increasing the likelihood of FAI development. From a structural perspective, increased α and CE angles as well as reduced femoral offset represent key anatomical characteristics underlying FAI syndrome. These features correspond to cam-type deformity characterized by femoral head-neck asphericity, pincer-type deformity characterized by excessive acetabular coverage, and insufficient femoral head-neck offset. These pathological patterns aggravate pathological mechanical conflict between the proximal femur and the acetabular margin, thus increasing the risk of FAI syndrome.

Research on the risk factors associated with FAI syndrome remains limited. Uzun et al. [23] reported old age, higher Tonnis grade, and full-thickness acetabular chondral lesions as risk factors of total hip replacement in patients with FAI syndrome. Ke et al. [24] further demonstrated that FAI subtypes, BMI, hip range of motion, and Tonnis classification are associated with the development of hip osteoarthritis after arthroscopy in FAI patients. Based on the results of multivariate analysis, an individualized predictive nomogram for FAI syndrome was constructed. The excellent high discriminatory power demonstrated by this model is mainly attributed to the inclusion of key imaging parameters (α angle, CE angle, and femoral offset), all of which are well-established diagnostic criteria for FAI syndrome. Therefore, the core value of this study lies in its integration of these established diagnostic criteria with clinical risk factors (such as old age and Hx_HIE) to build a visualized and quantitative tool for comprehensive risk assessment.

Conclusion

Combined imaging using X-ray, CT, and MRI demonstrates excellent diagnostic value for identifying FAI syndrome and its subtypes. Patients with clinical features such as age ≥32 years, history of high-intensity exercise, increased α and/or CE angle, and reduced femoral offset have an increased risk of developing FAI syndrome. Additionally, the constructed nomogram may serve as an effective tool to assist clinicians in identifying individuals at high risk of FAI syndrome.

Disclosure of conflict of interest

None.

Address correspondence to: Weiguo Zhang, Department of Radiology, Beijing Chao-Yang Hospital, Capital Medical University, No. 8, Gongti South Road, Chaoyang District, Beijing 100021, China. Tel: +86-010-85231091; E-mail: Zhangweiguo0906@sina.com

References

[1] Wang JC, Liu KC, Gettleman BS, Chen M, Piple AS, Yang J, Heckmann ND and Christ AB. Characteristics of very young patients undergoing total hip arthroplasty: a contemporary assessment. Arthroplast Today 2024; 25: 101268.

[2] Owen MM, Gohal C, Angileri HS, Hartwell MJ, Plantz MA, Tjong VK and Terry MA. Sex-based differences in prevalence, outcomes, and complications of hip arthroscopy for femoroacetabular impingement: a systematic review and meta-analysis. Orthop J Sports Med 2023; 11: 23259671231188332.

[3] Tey-Pons M, Sanchis-Alfonso V, Parra-Calabuig L, Griffin DR, Espregueira-Mendes J and Monllau JC. Anterior knee pain patients without structural knee abnormalities and normal lower limb skeletal alignment have a higher prevalence of cam-femoroacetabular impingement syndrome than the general population. J ISAKOS 2024; 9: 497-501.

[4] Mascarenhas VV, Rego P, Dantas P, Morais F, McWilliams J, Collado D, Marques H, Gaspar A, Soldado F and Consciencia JG. Imaging prevalence of femoroacetabular impingement in

symptomatic patients, athletes, and asymptomatic individuals: a systematic review. Eur J Radiol 2016; 85: 73-95.
[5] Pasculli RM, Callahan EA, Wu J, Edralin N and Berrigan WA. Non-operative management and outcomes of femoroacetabular impingement syndrome. Curr Rev Musculoskelet Med 2023; 16: 501-513.
[6] Lee DH, Park KT, Won J, An JH, Park JW and Lee YK. Epidemiology of femoroacetabular impingement in Korea. J Korean Med Sci 2025; 40: e124.
[7] Clohisy JC, Knaus ER, Hunt DM, Lesher JM, Harris-Hayes M and Prather H. Clinical presentation of patients with symptomatic anterior hip impingement. Clin Orthop Relat Res 2009; 467: 638-644.
[8] Fernandes DA, Martins EC, Melo G, Locks R, Adam GP and Neves FS. Diagnostic capability of intra-articular injections for femoroacetabular impingement syndrome: a systematic review. Clin J Sport Med 2024; 34: 615-623.
[9] Ou X, Chen X, Xu X, Xie L, Chen X, Hong Z, Bai H, Liu X, Chen Q, Li L and Yang H. Recent development in X-ray imaging technology: future and challenges. Research (Wash D C) 2021; 2021: 9892152.
[10] Sun H, Wang X, Li Z, Liu A, Xu S, Jiang Q, Li Q, Xue Z, Gong J, Chen L, Xiao Y and Liu S. Automated Rib fracture detection on chest X-Ray using contrastive learning. J Digit Imaging 2023; 36: 2138-2147.
[11] Kucukciloglu Y, Sekeroglu B, Adali T and Senturk N. Prediction of osteoporosis using MRI and CT scans with unimodal and multimodal deep-learning models. Diagn Interv Radiol 2024; 30: 9-20.
[12] Kijowski R and Fritz J. Emerging technology in musculoskeletal MRI and CT. Radiology 2023; 306: 6-19.
[13] Ryan ME and Jaju A. Revolutionizing pediatric neuroimaging: the era of CT, MRI, and beyond. Childs Nerv Syst 2023; 39: 2583-2592.
[14] Kim AYE, Lyons K, Sarmiento M, Lafage V and Iyer S. MRI-based score for assessment of bone mineral density in operative spine patients. Spine (Phila Pa 1976) 2023; 48: 107-112.
[15] Gomez-Verdejo F, Alvarado-Solorio E and Suarez-Ahedo C. Review of femoroacetabular impingement syndrome. J Hip Preserv Surg 2024; 11: 315-322.
[16] Colasanti CA, Shankar DS, Li ZI, Savage-Elliott I, Rynecki ND, Bi AS and Youm TJ. Effect of spinopelvic parameters on outcomes after hip arthroscopy for femoroacetabular impingement syndrome. Am J Sports Med 2024; 52: 1735-1743.
[17] Atalar E, Ureten K, Kanatli U, Ciceklidag M, Kaya I, Vural A and Maras Y. The diagnosis of femoroacetabular impingement can be made on pelvis radiographs using deep learning methods. Jt Dis Relat Surg 2023; 34: 298-304.
[18] Ferrero A, Powell GM, Adaaquah DK, Rajendran K, Thorne JE, Krych AJ, Horst KK, McCollough CH and Baffour FI. Feasibility of photon-counting CT for femoroacetabular impingement syndrome evaluation: lower radiation dose and improved diagnostic confidence. Skeletal Radiol 2023; 52: 1651-1659.
[19] Newhouse AC, Alter TD, Handoklow LA, Espinoza Orias AA, Inoue N and Nho SJ. 3.0T magnetic resonance imaging-based hip bone models for femoroacetabular impingement syndrome are equivalent to computed tomography-based models. J Orthop Res 2024; 42: 2017-2025.
[20] Xing Q, Feng X, Wan L, Cao H, Bai X and Wang S. MRI measurement assessment on ischiofemoral impingement syndrome. Hip Int 2023; 33: 119-125.
[21] Montin E, Kijowski R, Youm T and Lattanzi R. A radiomics approach to the diagnosis of femoroacetabular impingement. Front Radiol 2023; 3: 1151258.
[22] Hayashi S, Kuroda Y, Nakano N, Matsumoto T, Kamenaga T, Maeda T and Kuroda R. A combination of acetabular coverage and femoral head-neck measurements can help diagnose femoroacetabular impingement. J Hip Preserv Surg 2022; 9: 252-258.
[23] Uzun E, Ferrer-Rivero J, Lizano X, Cabello J, Gursu S and Pons MT. High satisfaction and low conversion rate to total hip arthroplasty after hip arthroscopy for femoroacetabular impingement syndrome and risk factors affecting survival at long-term follow-up. Knee Surg Sports Traumatol Arthrosc 2025; 33: 1507-1514.
[24] Ke L, Kou WG, Ma C, Zhang YZ and Liu DS. Risk factors for hip osteoarthritis after arthroscopy in patients with femoroacetabular impingement. Zhongguo Gu Shang 2024; 37: 179-183.